Research Paper
Computational Methods for Differential Equations
http://cmde.tabrizu.ac.ir
Vol. *, No. *, *, pp. 1-14
DOI:10.22034/cmde.2026.70317.3484

Rigorous stability analysis of a high-order fully discrete spectral scheme for multi-term time-fractional diffusion equations involving Riesz space-fractional operators

Meysam Asadipour, Hamid Rezaei, and MohammadHossein Derakhshan

Department of Mathematics, College of Sciences, Yasouj University, Yasouj-75914-74831, Iran.

Abstract

This study presented an effective hybrid numerical technique for obtaining approximate solutions to a multi-term time-fractional diffusion equation containing the Riesz space-fractional operator. In the proposed framework, the L1 discretization scheme and the Legendre spectral method were combined to handle the fractional model efficiently. The temporal component of the problem was approximated using the L1 scheme, whereas the spatial component was treated through the Legendre spectral technique, resulting in a fully discrete computational method. In addition, the stability and convergence properties of the developed numerical scheme were thoroughly analyzed. To validate the accuracy and performance of the proposed approach, a numerical experiment was included at the end of the study.

Keywords. Stability and convergence, L1 approximation, Riesz-space fractional operator, Legendre spectral approach.

2010 Mathematics Subject Classification. 26A33, 35R11, 65M12, 65D12.

1. Introduction

. The development of fractional calculus has followed a path similar to that of classical integer-order calculus; however, fractional calculus has gained considerable attention because of its distinctive features. A major reason for this interest is the non-local behavior of fractional operators, which sets them apart from traditional integer-order operators [2, 3, 5, 14, 15, 26, 31]. Researchers gradually discovered that fractional operators are capable of describing many complicated physical and engineering phenomena with higher accuracy. As a result, fractional differential equations emerged as an important research topic, since they provide mathematical models for processes that cannot be adequately represented through classical calculus. These equations have found extensive applications in physics, engineering, and applied mathematics. Among the many applications of fractional calculus, diffusion modeling has received significant attention. Diffusion equations are widely used to describe transport mechanisms and particle movement in different media [4, 28, 32, 36, 39, 40]. By incorporating fractional operators into diffusion models, researchers were able to capture anomalous diffusion behavior and memory-dependent effects more effectively. Various investigations have shown that fractional-order models possess greater adaptability and can produce more accurate results than conventional integer-order formulations. Therefore, fractional differential equations have become valuable tools for both theoretical investigations and real-world applications. In general, fractional calculus has proven to be a powerful extension of classical calculus, offering deeper understanding and improved modeling of complex natural and engineering systems.

Received: 19 November 2025; Accepted: 14 July 2026.
∗ Corresponding author. Email: rezaei@yu.ac.ir.

In the present work, we study a multi-term time-fractional diffusion equation containing the Riesz space-fractional operator, which can be expressed as

$$\begin{aligned}\sum_{k=1}^{q} p_k \, {}_0^C\mathrm{D}_t^{\beta_k} z(x,y,t) &= \frac{\mathcal{A}_x}{\Gamma(\alpha-1)} \int_0^t (t-\tau)^{\alpha-2} e^{-\theta(t-\tau)} \frac{\partial^\mu z(x,y,\tau)}{\partial |x|^\mu}\, d\tau \\ &+ \frac{\mathcal{A}_y}{\Gamma(\alpha-1)} \int_0^t (t-\tau)^{\alpha-2} e^{-\theta(t-\tau)} \frac{\partial^\nu z(x,y,\tau)}{\partial |y|^\nu}\, d\tau \\ &+ g(x,y,t), \quad (x,y) \in \Omega = (a_1,b_1)\times(a_2,b_2), \quad t \in (0,T]. \end{aligned} \tag{1.1}$$

The corresponding initial and boundary conditions are given by

$$\begin{aligned} &z(x,y,0) = z_0(x,y), \\ &z(x,y,t) = 0, \qquad (x,y) \in \partial\Omega, \quad t \in (0,T]. \end{aligned} \tag{1.2}$$

The parameters satisfy

$$0 < \beta_q < \cdots < \beta_2 < \beta_1 < 1, \qquad \mu,\nu,\alpha \in (1,2], \qquad \theta \geq 0,$$

where $\mathcal{A}_x$ and $\mathcal{A}_y$ are positive constants. The operator ${}_0^C\mathrm{D}_t^{\beta}$ denotes the Caputo fractional derivative of order β, defined by

$${}_0^C\mathrm{D}_t^{\beta} z(x,y,t) = \frac{1}{\Gamma(1-\beta)} \int_0^t (t-\tau)^{-\beta} \frac{\partial z(x,y,\tau)}{\partial \tau}\, d\tau. \tag{1.3}$$

Moreover, the Riesz space-fractional derivatives are defined as

$$\begin{aligned} \frac{\partial^\mu z(x,y,t)}{\partial |x|^\mu} &= -\frac{1}{2\cos\left(\frac{\mu\pi}{2}\right)} \left({}_a\mathcal{D}_x^\mu z(x,y,t) + {}_x\mathcal{D}_b^\mu z(x,y,t) \right), \\ \frac{\partial^\nu z(x,y,t)}{\partial |y|^\nu} &= -\frac{1}{2\cos\left(\frac{\nu\pi}{2}\right)} \left({}_c\mathcal{D}_y^\nu z(x,y,t) + {}_y\mathcal{D}_d^\nu z(x,y,t) \right). \end{aligned} \tag{1.4}$$

The left- and right-sided Riemann–Liouville fractional derivatives are given by

$$\begin{aligned} {}_a\mathcal{D}_x^\mu z(x,y,t) &= \frac{1}{\Gamma(2-\mu)} \frac{d^2}{dx^2} \int_a^x \frac{z(\tau,y,t)}{(x-\tau)^{\mu-1}}\, d\tau, \\ {}_x\mathcal{D}_b^\mu z(x,y,t) &= \frac{1}{\Gamma(2-\mu)} \frac{d^2}{dx^2} \int_x^b \frac{z(\tau,y,t)}{(\tau-x)^{\mu-1}}\, d\tau, \\ {}_c\mathcal{D}_y^\nu z(x,y,t) &= \frac{1}{\Gamma(2-\nu)} \frac{d^2}{dy^2} \int_c^y \frac{z(x,\tau,t)}{(y-\tau)^{\nu-1}}\, d\tau, \\ {}_y\mathcal{D}_d^\nu z(x,y,t) &= \frac{1}{\Gamma(2-\nu)} \frac{d^2}{dy^2} \int_y^d \frac{z(x,\tau,t)}{(\tau-y)^{\nu-1}}\, d\tau. \end{aligned} \tag{1.5}$$

In general, deriving exact analytical solutions for fractional differential equations is highly challenging because of the complexity introduced by fractional operators. Consequently, numerical techniques have become essential tools for obtaining approximate solutions of such models. Over the years, numerous computational approaches have been developed for different classes of fractional problems. For example, Odibat and Baleanu [30] introduced a generalized cardinal sine function approach for time-fractional equations. Jafari et al. [21] proposed a meshless finite difference framework for multi-term time-fractional models. Wei et al. [37] applied a local discontinuous Galerkin scheme to fractional advection–diffusion equations. Jia et al. [22] designed a fast computational algorithm based on the L1 discretization technique for time-fractional diffusion equations. In another work, Li et al. [25] utilized the L1-Galerkin finite element method to solve nonlinear time-fractional parabolic equations. In addition, Zayernouri and Karniadakis [38] employed a spectral element formulation for solving time- and space-fractional advection equations. Huang et al. [20] developed a fourth-order difference scheme for two-dimensional Riesz space-fractional diffusion models. Srivastava et al. [35] combined finite difference techniques with operational matrices to solve Riesz-space fractional partial differential equations. Zhu et al. [41] proposed a second-order ADI difference method for three-dimensional Riesz space-fractional diffusion equations. Abbaszadeh [1] investigated a second-order finite difference approach for the distributed-order Riesz space diffusion model. Derakhshan [8] presented a difference-Legendre spectral technique for two-dimensional Riesz space distributed-order diffusion-wave equations. Moreover, Ghazizadeh et al. [17] examined both explicit and implicit finite difference schemes for the fractional Cattaneo equation. Fouladi and Mohammadi Firouzjaei [16] also implemented a local discontinuous Galerkin method to solve the Riesz space distributed-order Sobolev equation. Altogether, these investigations demonstrate the broad applicability and effectiveness of numerical methods in solving complex fractional differential models. In recent years, the numerical treatment of fractional differential equations has attracted significant attention due to their ability to model memory and hereditary properties in complex physical systems. A wide variety of efficient and high-order numerical techniques have been developed to address challenges arising from nonlocality, weak singularities, and computational cost. Wavelet-based and spectral approaches have been widely used for solving fractional problems. For instance, wavelet Galerkin techniques have been successfully applied to fractional delay differential equations, providing high accuracy and flexibility in handling complex solution structures [19]. Similarly, cubic B-spline collocation and spline-based optimal control strategies have demonstrated strong performance in time-fractional diffusion and multi-delay control problems, offering both stability and computational efficiency [23, 24]. On the other hand, finite difference and finite element type methods remain fundamental tools in this area. Crank–Nicolson-based schemes combined with differential transformation methods have been developed for convection–diffusion–reaction equations, along with rigorous stability and truncation error analysis [18]. High-order numerical approximations for multi-dimensional time-fractional reaction–diffusion problems have also been proposed to effectively handle weak initial singularities [34]. Spectral and polynomial-based methods provide another powerful class of techniques. Chebyshev polynomial approaches have been used for coupled fractional integro-differential systems, showing good convergence properties and computational robustness [12]. In addition, Legendre and other orthogonal polynomial frameworks have been effectively employed for distributed-order fractional partial differential equations using advanced time discretization strategies such as GL1-2 schemes and second-order Riesz operators [13]. Furthermore, fractional optimal control problems have been extensively studied using wavelet and spline-based approaches. Efficient numerical frameworks based on cubic B-splines and wavelet expansions have been developed for multi-delay and Caputo–Katugampola type systems, demonstrating strong applicability in control theory and engineering problems [24, 29]. From a theoretical perspective, stability and asymptotic behavior of fractional systems remain crucial topics. Several works have addressed the stability of fractional differential systems and higher-order fractional multi-step methods, providing important theoretical foundations for numerical schemes [9, 27]. Moreover, comparisons between different numerical approaches, such as homotopy perturbation transform methods and fractional Adams–Bashforth schemes, have been carried out for nonlinear fractional models involving Prabhakar derivatives [10]. Overall, these studies highlight the continuous development of robust, accurate, and efficient numerical methods for fractional differential equations, covering a wide range of applications from diffusion-reaction systems to optimal control and integro-differential models [11].

The remainder of this manuscript is organized as follows. In Section 2, the numerical framework developed for approximating the proposed time-fractional diffusion model is presented in detail. First, a semi-discrete numerical formulation based on the L1 approximation technique is constructed to discretize the fractional derivative in the temporal direction. Subsequently, a Legendre spectral method is employed to approximate the spatial fractional operators, leading to the derivation of a fully discrete numerical scheme for the considered model. Furthermore, this section provides a comprehensive theoretical analysis of the proposed method, including the investigation of its stability and convergence properties, which confirms the reliability and robustness of the developed computational approach. Section 3 is devoted to numerical simulations and computational experiments. In this section, a representative test example is examined to demonstrate the applicability and effectiveness of the proposed method. The obtained numerical results are carefully analyzed in order to evaluate the accuracy, efficiency, and overall performance of the developed numerical scheme. Comparisons between the numerical approximations and the exact solutions, whenever available, are also presented to verify the validity of the method and illustrate its high level of precision. Finally, the manuscript concludes with a summary of the main contributions and significant findings obtained throughout the study. In addition, several possible extensions of the present work and potential directions for future investigations are discussed, particularly in relation to the development of more advanced numerical techniques and the application of the proposed approach to other classes of fractional differential equations.

2. Numerical approximation for the proposed time-fractional model

In this section, we construct a numerical framework for approximating the proposed multi-term time-fractional diffusion equation involving the Riesz space-fractional operator. The temporal fractional derivative is discretized using the L1 approximation method, while the spatial fractional operators are approximated by means of the Legendre spectral technique. Combining these approaches leads to a semi-discrete and subsequently a fully discrete numerical formulation for the considered model. To begin the temporal discretization, we introduce the following graded mesh:

$$t_l = T\left(\frac{l}{\mathcal{M}}\right)^j, \qquad j \geq 1, \qquad l = 0, 1, 2, \ldots, \mathcal{M}, \tag{2.1}$$

with

$$\Delta t_l = t_l - t_{l-1}, \qquad l = 1, 2, \ldots, \mathcal{M}.$$

Using the definition of the Caputo fractional derivative given in Eq. (1.3), the L1 approximation at the time level t_{n+1} is obtained as follows:

$$\begin{aligned}
\mathrm{D}^{\beta_k} z(x, y, t_{n+1}) &= \frac{1}{\Gamma(1-\beta_k)} \sum_{i=0}^{n} \frac{z^{i+1} - z^i}{\Delta t_{i+1}} \int_{t_i}^{t_{i+1}} (t_{n+1} - \tau)^{-\beta_k} \, d\tau \\
&= \frac{1}{\Gamma(2-\beta_k)} \sum_{i=0}^{n} \frac{(t_{n+1} - t_i)^{1-\beta_k} - (t_{n+1} - t_{i+1})^{1-\beta_k}}{\Delta t_{i+1}} (z^{i+1} - z^i) \\
&= \sum_{i=0}^{n} \mathcal{B}_{n,i}^k (z^{i+1} - z^i) \\
&= \mathcal{B}_{n,n}^k z^{n+1} - \sum_{i=1}^{n} \left(\mathcal{B}_{n,i}^k - \mathcal{B}_{n,i-1}^k\right) z^i - \mathcal{B}_{n,0}^k z^0,
\end{aligned} \tag{2.2}$$

where

$$\mathcal{B}_{n,i}^k = \frac{(t_{n+1} - t_i)^{1-\beta_k} - (t_{n+1} - t_{i+1})^{1-\beta_k}}{\Gamma(2-\beta_k)\,\Delta t_{i+1}}, \qquad n = 0, 1, \ldots, \mathcal{M} - 1. \tag{2.3}$$

Applying the mean value theorem gives

$$\frac{1-\beta_k}{\Gamma(2-\beta_k)} (t_{n+1} - t_i)^{-\beta_k} \leq \mathcal{B}_{n,i}^k \leq \frac{1-\beta_k}{\Gamma(2-\beta_k)} (t_{n+1} - t_{i+1})^{-\beta_k}. \tag{2.4}$$

Hence, the following properties hold:

$$\mathcal{B}_{n,0}^k \geq 0, \qquad \mathcal{B}_{n,i}^k \leq \mathcal{B}_{n,i+1}^k, \tag{2.5}$$

for

$$n = 0, 1, \ldots, \mathcal{M} - 1, \qquad i = 0, 1, \ldots, n.$$

These properties are important in establishing the stability and convergence of the numerical approximation.

Lemma 2.1. *[6] Suppose that $1 < \alpha \leq 2$ and $\theta \geq 0$. Then,*

$$\begin{aligned}
I_t^{\alpha-1,\theta} z(x, y, t)\Big|_{t=t_n} &= \frac{1}{\Gamma(\alpha-1)} \int_0^{t_n} (t_n - s)^{\alpha-2} e^{-\theta(t_n - s)} z(x, y, s) \, ds \\
&= (\Delta t)^{\alpha-1} \sum_{\iota=0}^{n} \vartheta_\iota^{\alpha-1} z(x, y, t_{n-\iota}) + \mathcal{O}\left((\Delta t)^2\right).
\end{aligned} \tag{2.6}$$

The coefficients $\vartheta_\iota^{\alpha-1}$ *are defined by*

$$\vartheta_\iota^{\alpha-1} = \left(\frac{3}{2}\right)^{1-\alpha} e^{-\theta\iota\Delta t} \sum_{\lambda=0}^{\iota} 3^{-\lambda} w_\lambda^{1-\alpha} w_{\iota-\lambda}^{1-\alpha}. \tag{2.7}$$

Lemma 2.2. *[7] Let*

$$(\varrho^0, \varrho^1, \dots, \varrho^{\mathcal{M}}) \in \mathbb{R}^{\mathcal{M}+1}.$$

Then, for $1 < \alpha \leq 2$, *the following inequality holds:*

$$\sum_{m=0}^{\mathcal{M}} \left[\sum_{\sigma=0}^{m} \vartheta_\sigma^\alpha \varrho^{m-\sigma}\right] \varrho^m \geq 0. \tag{2.8}$$

Therefore, the time-fractional diffusion equation in Eq. (1.1) at $t = t_{n+1}$ can be rewritten as

$$\sum_{k=1}^{q} p_k \, {}_0^C\mathrm{D}^{\beta_k} z^{n+1} = I_t^{\alpha-1,\theta} \left(\mathcal{A}_x \frac{\partial^\mu z^{n+1}}{\partial|x|^\mu} + \mathcal{A}_y \frac{\partial^\nu z^{n+1}}{\partial|y|^\nu}\right) + g^{n+1}, \tag{2.9}$$

where

$$z^{n+1} = z(x, y, t_{n+1}), \qquad g^{n+1} = g(x, y, t_{n+1}).$$

The operator $I_t^{\alpha-1,\theta}$ is defined as

$$\begin{aligned} I_t^{\alpha-1,\theta} \left(\mathcal{A}_x \frac{\partial^\mu z(x,y,t)}{\partial|x|^\mu} + \mathcal{A}_y \frac{\partial^\nu z(x,y,t)}{\partial|y|^\nu}\right) &= \frac{1}{\Gamma(\alpha-1)} \int_0^t (t-\tau)^{\alpha-2} e^{-\theta(t-\tau)} \mathcal{A}_x \frac{\partial^\mu z(x,y,\tau)}{\partial|x|^\mu} \, d\tau \\ &+ \frac{1}{\Gamma(\alpha-1)} \int_0^t (t-\tau)^{\alpha-2} e^{-\theta(t-\tau)} \mathcal{A}_y \frac{\partial^\nu z(x,y,\tau)}{\partial|y|^\nu} \, d\tau. \end{aligned} \tag{2.10}$$

Applying Lemma 2.1, we obtain the semi-discrete approximation

$$\sum_{k=1}^{q} p_k \, {}_0^C\mathrm{D}^{\beta_k} z^{n+1} \approx (\Delta t)^{\alpha-1} \sum_{\iota=0}^{n} \vartheta_\iota^{\alpha-1} \left(\mathcal{A}_x \frac{\partial^\mu z^{n-\iota+1}}{\partial|x|^\mu} + \mathcal{A}_y \frac{\partial^\nu z^{n-\iota+1}}{\partial|y|^\nu}\right) + g^{n+1} + \mathcal{O}\left((\Delta t)^2\right). \tag{2.11}$$

Substituting Eq. (2.2) into Eq. (2.11) yields

$$\begin{aligned} \sum_{k=1}^{q} p_k \, {}_0^C\mathrm{D}^{\beta_k} z^{n+1} &= \sum_{k=1}^{q} p_k \left[\mathcal{B}_{n,n}^k z^{n+1} - \sum_{i=1}^{n} \left(\mathcal{B}_{n,i}^k - \mathcal{B}_{n,i-1}^k\right) z^i - \mathcal{B}_{n,0}^k z^0\right] \\ &= (\Delta t)^{\alpha-1} \sum_{\iota=0}^{n} \vartheta_\iota^{\alpha-1} \left(\mathcal{A}_x \frac{\partial^\mu z^{n-\iota+1}}{\partial|x|^\mu} + \mathcal{A}_y \frac{\partial^\nu z^{n-\iota+1}}{\partial|y|^\nu}\right) + g^{n+1} + \mathcal{O}\left((\Delta t)^2\right). \end{aligned} \tag{2.12}$$

Finally, solving for z^{n+1}, we obtain

$$z^{n+1} = \frac{(\Delta t)^{\alpha-1} \sum_{\iota=0}^{n} \vartheta_\iota^{\alpha-1} \left(\mathcal{A}_x \frac{\partial^\mu z^{n-\iota+1}}{\partial|x|^\mu} + \mathcal{A}_y \frac{\partial^\nu z^{n-\iota+1}}{\partial|y|^\nu}\right) + g^{n+1} + \sum_{k=1}^{q} p_k \sum_{i=1}^{n} \left(\mathcal{B}_{n,i}^k - \mathcal{B}_{n,i-1}^k\right) z^i + \sum_{k=1}^{q} p_k \mathcal{B}_{n,0}^k z^0}{\sum_{k=1}^{q} p_k \mathcal{B}_{n,n}^k}. \tag{2.13}$$

Equation (2.13) represents the semi-discrete numerical approximation in the temporal direction. In the next step, the Legendre spectral method is employed to discretize the spatial fractional operators and derive the fully discrete numerical scheme for the proposed fractional diffusion model. To discretize the spatial variables appearing in Eq. (1.1), we employ a highly accurate numerical technique based on the Legendre spectral method. Spectral methods are widely used for solving fractional partial differential equations because of their excellent convergence properties and high computational efficiency, especially when the exact solution possesses sufficient smoothness. In the present work, suitable basis functions are constructed from Legendre polynomials in order to satisfy the homogeneous boundary conditions naturally and to provide an accurate approximation of the spatial fractional operators. We introduce the following basis functions:

$$\begin{aligned}
\varphi_k^{(1)}(x) &= \mathrm{L}_k(\hat{x}) - \mathrm{L}_{k+2}(\hat{x}), \qquad -1 \le \hat{x} \le 1, \\
x &= \frac{\mathbb{L}\hat{x} + \mathbb{L}}{2} \in [0, \mathbb{L}], \\
\varphi_k^{(2)}(y) &= \mathrm{L}_k(\hat{y}) - \mathrm{L}_{k+2}(\hat{y}), \qquad -1 \le \hat{y} \le 1, \\
y &= \frac{\mathbb{L}\hat{y} + \mathbb{L}}{2} \in [0, \mathbb{L}],
\end{aligned} \tag{2.14}$$

where

$$k = 0, 1, 2, \ldots, \mathcal{N},$$

and $\mathrm{L}_k(\cdot)$ denotes the Legendre polynomial of degree k.

The Legendre polynomials satisfy the following recursive relations [33]:

$$\begin{aligned}
&\mathrm{L}_0(\hat{x}) = 1, \qquad \mathrm{L}_1(\hat{x}) = \hat{x}, \\
&\mathrm{L}_{k+1}(\hat{x}) = \frac{(2k+1)\hat{x}}{k+1}\mathrm{L}_k(\hat{x}) - \frac{k}{k+1}\mathrm{L}_{k-1}(\hat{x}), \qquad k \ge 1, \\
&(1 - \hat{x}^2)\mathrm{L}_k'(\hat{x}) = \frac{k(k+1)}{2k+1}\Big(\mathrm{L}_{k-1}(\hat{x}) - \mathrm{L}_{k+1}(\hat{x})\Big), \\
&(2k+1)\mathrm{L}_k(\hat{x}) = \mathrm{L}_{k+1}'(\hat{x}) - \mathrm{L}_{k-1}'(\hat{x}).
\end{aligned} \tag{2.15}$$

Using Eqs. (2.14) and (2.17), the derivatives of the basis functions are obtained as

$$\frac{d}{dx}\varphi_k^{(1)}(x) = -(2k+3)\mathrm{L}_{k+1}(\hat{x}), \qquad \frac{d}{dy}\varphi_k^{(2)}(y) = -(2k+3)\mathrm{L}_{k+1}(\hat{y}). \tag{2.16}$$

Next, we define the finite-dimensional spectral space associated with the Legendre approximation as follows:

$$\mathrm{S}_{\mathcal{N}} = \mathrm{Span}\left\{\varphi_k^{(1)}(x)\varphi_{k'}^{(2)}(y) \;:\; x, y \in [0, \mathbb{L}], \quad k, k' = 0, 1, \ldots, \mathcal{N} - 2\right\}. \tag{2.17}$$

Therefore, any approximate solution belonging to the spectral space $\mathrm{S}_{\mathcal{N}}$ can be expressed as a finite expansion in terms of the tensor-product Legendre basis functions:

$$z_{\mathcal{N}}^{n+1}(x, y) = \sum_{k=0}^{\mathcal{N}-2}\sum_{k'=0}^{\mathcal{N}-2} c_{k,k'}^{n+1}\,\varphi_k^{(1)}(x)\varphi_{k'}^{(2)}(y), \tag{2.18}$$

where $c_{k,k'}^{n+1}$ are the unknown spectral coefficients at time level t_{n+1}. In practice, these coefficients are not computed explicitly from the expansion formula, but are determined by enforcing the fully discrete weak formulation (2.21). This is achieved by substituting the spectral expansion into the numerical scheme and choosing the test function $\eta = \varphi_m^{(1)}(x)\varphi_{m'}^{(2)}(y)$, which leads to a linear algebraic system for the coefficients. Specifically, we obtain

$$\mathbf{A}\,\mathbf{c}^{\,n+1} = \mathbf{F}^{\,n+1} + \mathbf{G}^{\,n+1}(\mathbf{c}^{\,n}, \mathbf{c}^{\,n-1}, \ldots), \tag{2.19}$$

where $\mathbf{c}^{\,n+1} = \{c_{k,k'}^{n+1}\}$ is the vector of unknown coefficients, $\mathbf{A}$ is the stiffness-mass matrix arising from the fractional bilinear form $\mathcal{E}(\cdot,\cdot)$, and $\mathbf{F}^{\,n+1}$ corresponds to the projection of the source term $\mathcal{I}_{\mathcal{N}}g^{n+1}$. The term $\mathbf{G}^{\,n+1}$ collects all contributions from previous time levels induced by the multi-term fractional temporal discretization. More explicitly, each coefficient is obtained from the Galerkin condition

$$\left\langle z_{\mathcal{N}}^{n+1}, \varphi_m^{(1)}\varphi_{m'}^{(2)}\right\rangle = \sum_{k=0}^{\mathcal{N}-2}\sum_{k'=0}^{\mathcal{N}-2} c_{k,k'}^{n+1}\left\langle \varphi_k^{(1)}\varphi_{k'}^{(2)}, \varphi_m^{(1)}\varphi_{m'}^{(2)}\right\rangle, \tag{2.20}$$

which results in a structured system due to the orthogonality of the Legendre basis. Consequently, the coefficients $c_{k,k'}^{n+1}$ are obtained by solving a sparse linear system at each time step, where the system matrix remains constant in time and only the right-hand side changes due to the fractional history terms. Using the above approximation space, the fully discrete spectral formulation of the proposed time-fractional diffusion model is written as

$$\sum_{k=1}^{q} p_k \left\langle {}_0^C\mathrm{D}^{\beta_k} z_{\mathcal{N}}^{n+1}, \eta \right\rangle + (\Delta t)^{\alpha-1} \sum_{\iota=0}^{n} \vartheta_\iota^{\alpha-1} \mathcal{E}\left\langle z_{\mathcal{N}}^{n-\iota+1}, \eta \right\rangle = \left\langle \mathcal{I}_{\mathcal{N}} g^{n+1}, \eta \right\rangle + \mathcal{O}\big((\Delta t)^2\big), \qquad \forall\, \eta \in \mathrm{S}_{\mathcal{N}}. \tag{2.21}$$

$$z_{\mathcal{N}}^0 = \Pi_{\mathcal{N}}^{1,0} z_0. \tag{2.22}$$

Here, $\mathcal{I}_{\mathcal{N}}$ denotes the Legendre–Gauss interpolation operator, while $\mathcal{E}\langle \cdot, \cdot \rangle$ represents the bilinear form associated with the Riesz fractional spatial operators. This bilinear form is defined by

$$\begin{aligned} \mathcal{E}\langle z, z_1 \rangle = {} & \frac{\mathcal{A}_x}{2\cos\left(\frac{\mu\pi}{2}\right)} \Big(\langle {}_a\mathcal{D}_x^{\mu/2} z, {}_x\mathcal{D}_b^{\mu/2} z_1 \rangle + \langle {}_x\mathcal{D}_b^{\mu/2} z, {}_a\mathcal{D}_x^{\mu/2} z_1 \rangle \Big) \\ & + \frac{\mathcal{A}_y}{2\cos\left(\frac{\nu\pi}{2}\right)} \Big(\langle {}_c\mathcal{D}_y^{\nu/2} z, {}_y\mathcal{D}_d^{\nu/2} z_1 \rangle + \langle {}_y\mathcal{D}_d^{\nu/2} z, {}_c\mathcal{D}_y^{\nu/2} z_1 \rangle \Big). \end{aligned} \tag{2.23}$$

$$\left\langle \Pi_{\mathcal{N}}^{1,0} z - z, \eta \right\rangle + \left\langle \partial_x \left(\Pi_{\mathcal{N}}^{1,0} z - z \right), \partial_x \eta \right\rangle = 0, \qquad \forall\, \eta \in \mathrm{S}_{\mathcal{N}}. \tag{2.24}$$

In addition, the projection operator $\Pi_{\mathcal{N}}^{1,0}$ satisfies the following approximation estimate [39]:

$$\left\| z - \Pi_{\mathcal{N}}^{1,0} z \right\|_\tau \le C \mathcal{N}^{\tau - s} \|z\|_s, \qquad \tau = 0, 1, \qquad s \ge 1, \tag{2.25}$$

where C is a positive constant independent of Δt_n, n, and $\mathcal{N}$. Substituting the L1 approximation given in Eq. (2.2) into Eq. (2.21), we obtain

$$\begin{aligned} \sum_{k=1}^{q} p_k \mathcal{B}_{n,n}^k \left\langle z_{\mathcal{N}}^{n+1}, \eta \right\rangle + (\Delta t)^{\alpha-1} \sum_{\iota=0}^{n} \vartheta_\iota^{\alpha-1} \mathcal{E}\left\langle z_{\mathcal{N}}^{n-\iota+1}, \eta \right\rangle = {} & \sum_{k=1}^{q} \sum_{i=1}^{n} p_k \left(\mathcal{B}_{n,i}^k - \mathcal{B}_{n,i-1}^k \right) \left\langle z_{\mathcal{N}}^i, \eta \right\rangle \\ & + \sum_{k=1}^{q} p_k \mathcal{B}_{n,0}^k \left\langle z_{\mathcal{N}}^0, \eta \right\rangle + \left\langle \mathcal{I}_{\mathcal{N}} g^{n+1}, \eta \right\rangle + \mathcal{O}\big((\Delta t)^2\big), \qquad \forall\, \eta \in \mathrm{S}_{\mathcal{N}}. \end{aligned} \tag{2.26}$$

Neglecting the truncation term $\mathcal{O}((\Delta t)^2)$, let $Z_{\mathcal{N}}^i$ denote the approximate numerical solution of the fully discrete scheme. Then, the resulting formulation becomes

$$\begin{aligned} \sum_{k=1}^{q} p_k \mathcal{B}_{n,n}^k \left\langle Z_{\mathcal{N}}^{n+1}, \eta \right\rangle + (\Delta t)^{\alpha-1} \sum_{\iota=0}^{n} \vartheta_\iota^{\alpha-1} \mathcal{E}\left\langle Z_{\mathcal{N}}^{n-\iota+1}, \eta \right\rangle = {} & \sum_{k=1}^{q} \sum_{i=1}^{n} p_k \left(\mathcal{B}_{n,i}^k - \mathcal{B}_{n,i-1}^k \right) \left\langle Z_{\mathcal{N}}^i, \eta \right\rangle \\ & + \sum_{k=1}^{q} p_k \mathcal{B}_{n,0}^k \left\langle Z_{\mathcal{N}}^0, \eta \right\rangle + \left\langle \mathcal{I}_{\mathcal{N}} g^{n+1}, \eta \right\rangle, \qquad \forall\, \eta \in \mathrm{S}_{\mathcal{N}}. \end{aligned} \tag{2.27}$$

Finally, subtracting Eq. (2.26) from Eq. (2.27) and defining the error function

$$E^n = Z_{\mathcal{N}}^n - z_{\mathcal{N}}^n,$$

we arrive at the following error equation:

$$\begin{aligned} & \sum_{k=1}^{q} p_k \mathcal{B}_{n,n}^k \left\langle E^{n+1}, \eta \right\rangle + (\Delta t)^{\alpha-1} \sum_{\iota=0}^{n} \vartheta_\iota^{\alpha-1} \mathcal{E}\left\langle E^{n-\iota+1}, \eta \right\rangle = \sum_{k=1}^{q} \sum_{i=1}^{n} p_k \left(\mathcal{B}_{n,i}^k - \mathcal{B}_{n,i-1}^k \right) \left\langle E^i, \eta \right\rangle + \sum_{k=1}^{q} p_k \mathcal{B}_{n,0}^k \left\langle E^0, \eta \right\rangle, \\ & \forall\, \eta \in \mathrm{S}_{\mathcal{N}}, \qquad n = 0, 1, 2, \ldots, \mathcal{M} - 1. \end{aligned} \tag{2.28}$$

For the special case $n = 0$, Eq. (2.28) reduces to

$$\sum_{k=1}^{q} p_k \mathcal{B}_{0,0}^k \left\langle E^1, \eta \right\rangle + (\Delta t)^{\alpha-1} \vartheta_0^{\alpha-1} \mathcal{E}\left\langle E^1, \eta \right\rangle = \sum_{k=1}^{q} p_k \mathcal{B}_{0,0}^k \left\langle E^0, \eta \right\rangle.$$

In the next subsection, the stability analysis of the proposed fully discrete numerical method will be established by applying the principle of mathematical induction together with the positivity properties of the convolution coefficients.

Theorem 2.3. *(Stability analysis) The fully-discrete numerical scheme (2.28) obtained by the proposed method is unconditionally stable. Moreover, the stability estimate remains valid in the presence of the forcing term. Specifically, for all $n \in \mathbb{N} \cup \{0\}$, the numerical error satisfies*

$$\| E^{n+1} \| \leq \| E^0 \| + \mathbb{C} \max_{0 \leq m \leq n+1} \| g^m \|, \tag{2.29}$$

where $\mathbb{C}$ is a positive constant independent of Δt and $\mathcal{N}$. In the particular case of homogeneous forcing, namely $g = 0$, relation (2.29) reduces to

$$\| E^{n+1} \| \leq \| E^0 \| .$$

Proof. The proof is established by applying the mathematical induction principle. We first consider the case $n = 0$. Choosing the test function $\eta = E^1$ in Eq. (2.28), we obtain

$$\sum_{k=1}^{q} p_k \mathcal{B}_{0,0}^{k} \left\langle E^1, E^1 \right\rangle + (\Delta t)^{\alpha-1} \vartheta_0^{\alpha-1} \mathcal{E} \left\langle E^1, E^1 \right\rangle = \sum_{k=1}^{q} p_k \mathcal{B}_{0,0}^{k} \left\langle E^0, E^1 \right\rangle. \tag{2.30}$$

Using the definition of the bilinear form $\mathcal{E}\langle \cdot, \cdot \rangle$, we have

$$\begin{aligned}(\Delta t)^{\alpha-1} \vartheta_0^{\alpha-1} \mathcal{E} \left\langle E^1, E^1 \right\rangle &= (\Delta t)^{\alpha-1} \vartheta_0^{\alpha-1} \left(2\cos\left(\frac{\mu\pi}{2}\right)\right)^{-1} \mathcal{A}_x \Big(({}_a\mathcal{D}_x^{\frac{\mu}{2}} E^1, {}_x\mathcal{D}_b^{\frac{\mu}{2}} E^1) + ({}_x\mathcal{D}_b^{\frac{\mu}{2}} E^1, {}_a\mathcal{D}_x^{\frac{\mu}{2}} E^1) \Big) \\ &+ (\Delta t)^{\alpha-1} \vartheta_0^{\alpha-1} \left(2\cos\left(\frac{\nu\pi}{2}\right)\right)^{-1} \mathcal{A}_y \Big(({}_c\mathcal{D}_y^{\frac{\nu}{2}} E^1, {}_y\mathcal{D}_d^{\frac{\nu}{2}} E^1) + ({}_y\mathcal{D}_d^{\frac{\nu}{2}} E^1, {}_c\mathcal{D}_y^{\frac{\nu}{2}} E^1) \Big). \end{aligned} \tag{2.31}$$

From Lemma 2.2, the bilinear form is nonnegative. Consequently,

$$(\Delta t)^{\alpha-1} \vartheta_0^{\alpha-1} \mathcal{E} \left\langle E^1, E^1 \right\rangle \geq 0. \tag{2.32}$$

Substituting relation (2.32) into Eq. (2.30) and applying the Cauchy–Schwarz inequality yield

$$\sum_{k=1}^{q} p_k \mathcal{B}_{0,0}^{k} \| E^1 \|^2 \leq \sum_{k=1}^{q} p_k \mathcal{B}_{0,0}^{k} \| E^0 \| \| E^1 \| . \tag{2.33}$$

Hence,

$$\| E^1 \| \leq \| E^0 \| .$$

Assume now that the estimate

$$\| E^{\gamma+1} \| \leq \| E^0 \| + \mathbb{C} \max_{0 \leq m \leq \gamma+1} \| g^m \|$$

holds for $\gamma = 0, 1, \ldots, n-1$. For the case $\gamma = n$, taking $\eta = E^{n+1}$ in Eq. (2.28), we obtain

$$\begin{aligned}\sum_{k=1}^{q} p_k \mathcal{B}_{n,n}^{k} \left\langle E^{n+1}, E^{n+1} \right\rangle &+ (\Delta t)^{\alpha-1} \sum_{\iota=0}^{n} \vartheta_\iota^{\alpha-1} \mathcal{E} \left\langle E^{n-\iota+1}, E^{n+1} \right\rangle \\ &= \sum_{k=1}^{q} \sum_{i=1}^{n} p_k \big(\mathcal{B}_{n,i}^{k} - \mathcal{B}_{n,i-1}^{k} \big) \left\langle E^i, E^{n+1} \right\rangle + \sum_{k=1}^{q} p_k \mathcal{B}_{n,0}^{k} \left\langle E^0, E^{n+1} \right\rangle. \end{aligned} \tag{2.34}$$

Using again the positivity of the bilinear form $\mathcal{E}\langle \cdot, \cdot \rangle$, together with Lemma 2.2, we obtain

$$(\Delta t)^{\alpha-1} \sum_{\iota=0}^{n} \vartheta_\iota^{\alpha-1} \mathcal{E} \left\langle E^{n-\iota+1}, E^{n+1} \right\rangle \geq 0. \tag{2.35}$$

Therefore, Eq. (2.34) implies

$$\sum_{k=1}^{q} p_k \mathcal{B}_{n,n}^{k} \| E^{n+1} \|^2 \leq \sum_{k=1}^{q} \sum_{i=1}^{n} p_k \big(\mathcal{B}_{n,i}^{k} - \mathcal{B}_{n,i-1}^{k} \big) \| E^i \| \| E^{n+1} \| + \sum_{k=1}^{q} p_k \mathcal{B}_{n,0}^{k} \| E^0 \| \| E^{n+1} \| . \tag{2.36}$$

Dividing both sides by $\| E^{n+1} \|$ and applying the induction hypothesis lead to

$$\sum_{k=1}^{q} p_k \mathcal{B}_{n,n}^k \| E^{n+1} \| \leq \sum_{k=1}^{q} \sum_{i=1}^{n} p_k \big(\mathcal{B}_{n,i}^k - \mathcal{B}_{n,i-1}^k\big) \Big(\| E^0 \| + \mathbb{C} \max_{0 \leq m \leq i} \| g^m \| \Big) + \sum_{k=1}^{q} p_k \mathcal{B}_{n,0}^k \| E^0 \| . \tag{2.37}$$

Since the coefficients $\mathcal{B}_{n,i}^k$ are nonnegative and monotone, we obtain

$$\| E^{n+1} \| \leq \| E^0 \| + \mathbb{C} \max_{0 \leq m \leq n+1} \| g^m \| .$$

Hence, the fully-discrete numerical method is unconditionally stable. In particular, when the forcing term vanishes, the estimate reduces to

$$\| E^{n+1} \| \leq \| E^0 \|,$$

which completes the proof. □

3. Implementation and Numerical Simulation

In this section, several numerical examples are presented to demonstrate the efficiency and accuracy of the proposed fully discrete algorithm. The algorithm combines the L1 approximation in time with the Legendre spectral method in space. To accelerate the computation of the first term in equation (1.1), a fast algorithm based on the sum-of-exponentials (SOE) approach is applied. For reproducibility, we emphasize that the SOE approximation is constructed by approximating the weakly singular kernel $t^{-\beta_k}$ on a truncated interval using a finite sum of exponential functions with optimized quadrature nodes and weights, which are precomputed once at the beginning of the simulation. Under this approach, the Caputo fractional derivative in time can be decomposed into a local term and a history term as follows:

$$\begin{aligned} {}_0^C\mathrm{D}_t^{\beta_k} z(x,y,t_n) &= \frac{1}{\Gamma(\beta_k - 1)} \int_{t_{n-1}}^{t_n} \big(t_n - \tau\big)^{-\beta_k} \frac{\partial z(x,y,\tau)}{\partial \tau}\, d\tau + \frac{1}{\Gamma(\beta_k - 1)} \int_0^{t_{n-1}} \big(t_n - \tau\big)^{-\beta_k} \frac{\partial z(x,y,\tau)}{\partial \tau}\, d\tau \\ &= \mathcal{C}_l^n + \mathcal{C}_h^n, \end{aligned} \tag{3.1}$$

where $\mathcal{C}_l^n = \mathcal{C}_l(t_n)$ is the local term and $\mathcal{C}_h^n = \mathcal{C}_h(t_n)$ is the history term. These terms are approximated as

$$\begin{aligned} \mathcal{C}_l^n &\approx \big(\Delta t_n \Gamma(\beta_k - 1)\big)^{-1} \big(z^n - z^{n-1}\big) \int_{t_{n-1}}^{t_n} \big(t_n - \tau\big)^{-\beta_k}\, d\tau, \\ \mathcal{C}_h^n &\approx \big(\Gamma(\beta_k - 1)\big)^{-1} \Big\{ \big(\Delta t_{n-1}^{\beta_k}\big)^{-1} z^{n-1} - \big(t_n^{\beta_k}\big)^{-1} z^0 - \beta_k \sum_{j=1}^{\mathcal{N}_{exp}} \delta_j \mathcal{U}_{history}^n \Big\}, \end{aligned} \tag{3.2}$$

with the history variable $\mathcal{U}_{history}(t_n) = \mathcal{U}_{history}^n$ defined recursively by

$$\mathcal{U}_{history}^n = \exp\Big(-\tau_j \Delta t_{n-1} \Big) \mathcal{U}_{history}^{n-1} + \int_{t_{n-1}}^{t_{n-2}} \exp\Big(-\tau_j (t_n - y) \Big) z(y)\, dy. \tag{3.3}$$

In practical implementation, the recursion in (3.3) is evaluated in an online manner, where only a fixed number of past history variables is stored, reducing the computational cost from $\mathcal{O}(n^2)$ to approximately $\mathcal{O}(n \log n)$ depending on the SOE compression strategy. To evaluate the convergence behavior of the proposed algorithm, the convergence orders in time and space are defined as

$$\begin{aligned} CO_{Time} &= \Big(\log \Big\{ \frac{\Delta t_1}{\Delta t_2} \Big\} \Big)^{-1} \log \Big(\frac{AE\big(\Delta t_1\big)}{AE\big(\Delta t_2\big)} \Big), \\ CO_{Space} &= \Big(\log \Big\{ \frac{\mathcal{N}_2}{\mathcal{N}_1} \Big\} \Big)^{-1} \log \Big(\frac{AE\big(\mathcal{N}_1\big)}{AE\big(\mathcal{N}_2\big)} \Big), \end{aligned} \tag{3.4}$$

where the absolute error is $AE = \|z - z_{\mathcal{N}}^n\|$, and $\Delta t_1 \neq \Delta t_2$, $\mathcal{N}_1 \neq \mathcal{N}_2$. Here, the convergence rates are computed using successive mesh refinement in both temporal and spatial discretizations to ensure consistency with the theoretical error estimates derived in Section 4. All numerical simulations were performed using MATLAB 2018b, and the results

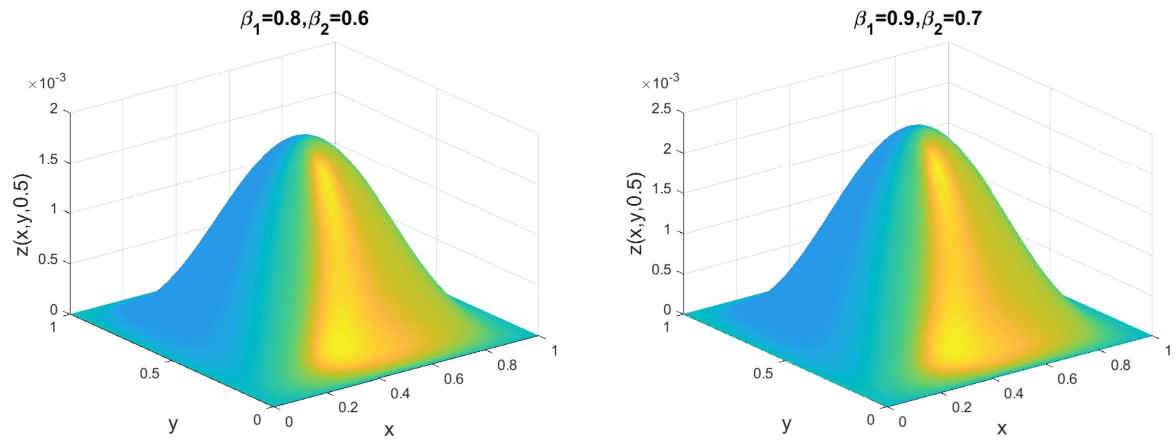

FIGURE 1. Graph of the approximate solution for Example 3.1 for different values of β_1 and β_2 with the values $p_2 = 0.35$, $\alpha = 1.5$, $\mu = 1.25$, $\nu = 1.75$ and $\theta = 0.1$.

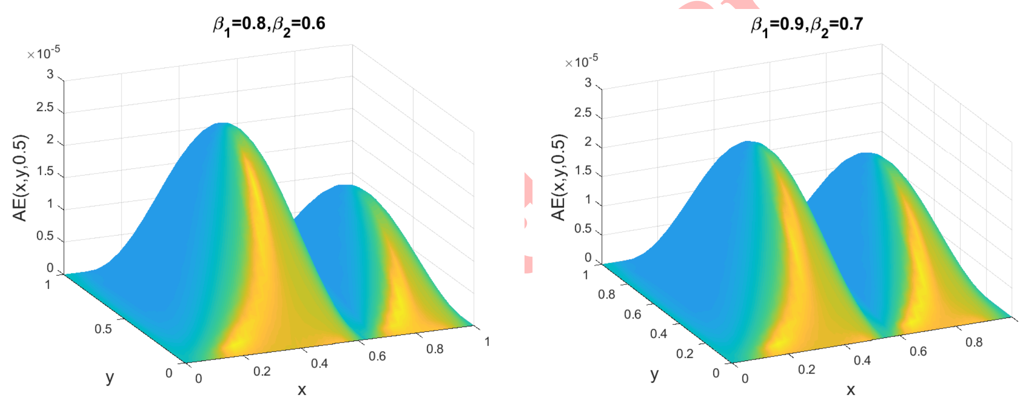

FIGURE 2. Graph of the error function for Example 3.1 with different values of β_1 and β_2 with the values $p_2 = 0.35$, $\alpha = 1.5$, $\mu = 1.25$, $\nu = 1.75$ and $\theta = 0.1$.

demonstrate that the proposed fast algorithm efficiently computes the time-fractional operator while maintaining high accuracy. These simulations also confirm the theoretical convergence orders and highlight the practicality of the method for solving multi-term time-fractional diffusion problems. A complete pseudocode of the SOE-based fast convolution algorithm is provided in Section 3 to ensure full reproducibility of the implementation.

Example 3.1. We study the two-dimensional time-fractional diffusion model of multi-term order involving the Riesz-space fractional operator as

$$
\begin{aligned}
{}_0^C\mathrm{D}_t^{\beta_1} z(x,y,t) + p_2 {}_0^C\mathrm{D}_t^{\beta_2} z(x,y,t) &= 0.5\frac{1}{\Gamma(\alpha-1)}\int_0^t (t-\tau)^{\alpha-2}\exp\big(-\theta\big(t-\tau\big)\big)\frac{\partial^\mu z(x,y,\tau)}{\partial|x|^\mu}\,d\tau \\
&\quad + 0.8\frac{1}{\Gamma(\alpha-1)}\int_0^t (t-\tau)^{\alpha-2}\exp\big(-\theta\big(t-\tau\big)\big)\frac{\partial^\nu z(x,y,\tau)}{\partial|y|^\nu}d\tau + g(x,y,t), \qquad (3.5)
\end{aligned}
$$

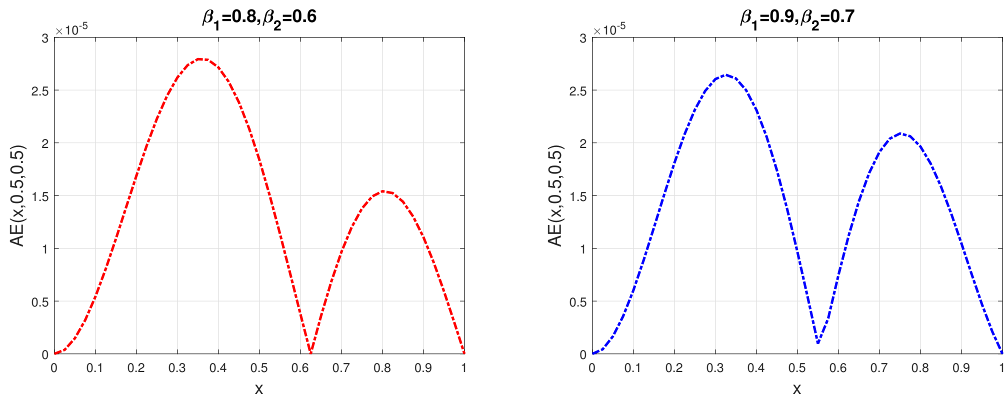

FIGURE 3. Graph of the error function for Example 3.1 with different values of β_1 and β_2 with the values $p_2 = 0.35$, $\alpha = 1.5$, $\mu = 1.25$, $\nu = 1.75$ and $\theta = 0.1$ at point $t = y = 0.5$.

TABLE 1. Comparison of the absolute error AE, temporal convergence order CO_{Time}, and CPU time (seconds) between the proposed method and a fast algorithm for Example 3.1 with $\beta_1 = 0.8$, $\beta_2 = 0.6$, and $\mathcal{N} = 64$.

$\mathcal{M}$	AE (Proposed)	CO_{Time}	CPU$_1$(s)	AE (Fast)	CO_{Time}	CPU$_2$(s)
$\frac{1}{32}$	6.84×10^{-6}	–	24.12	6.95×10^{-6}	–	23.05
$\frac{1}{64}$	1.74×10^{-6}	1.97	40.38	1.82×10^{-6}	1.94	38.71
$\frac{1}{128}$	4.42×10^{-7}	1.98	72.63	4.63×10^{-7}	1.95	69.48
$\frac{1}{256}$	1.12×10^{-7}	1.99	136.85	1.18×10^{-7}	1.97	131.22
$\frac{1}{512}$	2.83×10^{-8}	2.01	255.47	3.01×10^{-8}	1.98	247.66

under the given conditions by:

$$\begin{aligned} &z(x,y,0) = 0,\\ &z(x,y,t) = 0,\ (x,y) \in \Omega = [0,1] \times [0,1],\ 0 < t \leq 1. \end{aligned} \tag{3.6}$$

Here

$$\begin{aligned} g(x,y,t) = 10\Big\{&\Gamma(\beta_1+1) + \frac{6}{\Gamma(4-\beta_1)} t^{3-\beta_1} + \big(-\theta\big)^{\beta_1}\big(t^{\beta_1} + t^3\big) + p_2\Big(\frac{\Gamma(\beta_1+1)}{\Gamma(\beta_1-\beta_2+1)} t^{\beta_1-\beta_2}\\ &+ \frac{6}{\Gamma(4-\beta_2)} t^{3-\beta_2} + \big(-\theta\big)^{\beta_2}\big(t^{\beta_1} + t^3\big)\Big)\Big\} \exp\big(-\theta t\big)\big(xy(1-x)(1-y)\big)^2\\ &+ \Big\{\frac{\Gamma(\beta_1+1)}{\Gamma(\beta_1+\alpha)} t^{\beta_1+\alpha-1} + \frac{6}{\Gamma(3+\alpha)} t^{2-\alpha}\Big\} \frac{\big(y(1-y)\big)^2}{\cos\big(\frac{\pi\mu}{2}\big)} \Big(\frac{x^{2-\mu} + (1-x)^{2-\mu}}{\Gamma(3-\mu)} - 6\frac{x^{3-\mu} + (1-x)^{3-\mu}}{\Gamma(4-\mu)}\\ &+ 12\frac{x^{4-\mu} + (1-x)^{4-\mu}}{\Gamma(5-\mu)}\Big)\\ &+ \Big\{\frac{\Gamma(\beta_1+1)}{\Gamma(\beta_1+\alpha)} t^{\beta_1+\alpha-1} + \frac{6}{\Gamma(3+\alpha)} t^{2-\alpha}\Big\} \frac{\big(x(1-x)\big)^2}{\cos\big(\frac{\pi\nu}{2}\big)} \Big(\frac{y^{2-\nu} + (1-y)^{2-\nu}}{\Gamma(3-\nu)} - 6\frac{y^{3-\nu} + (1-y)^{3-\nu}}{\Gamma(4-\nu)}\\ &+ 12\frac{y^{4-\nu} + (1-y)^{4-\nu}}{\Gamma(5-\nu)}\Big). \end{aligned} \tag{3.7}$$

For this test problem, the exact solution is defined as

$$z(x,y,t) = 10\big(t^{\beta_1} + t^3\big)\exp(-\theta t)\big(xy(1-x)(1-y)\big)^2. \tag{3.8}$$

We solved this problem using the fully discrete numerical scheme developed in this study, which combines the L1 approximation in time with the Legendre spectral method in space. The numerical simulations were performed for different values of the fractional orders β_1 and β_2, while keeping the other parameters fixed as $p_2 = 0.35$, $\alpha = 1.5$, $\mu = 1.25$, $\nu = 1.75$, and $\theta = 0.1$. The purpose of these simulations was not only to verify the accuracy and stability of the proposed method but also to demonstrate the effect of varying fractional orders on the diffusion process. The obtained numerical results are illustrated in figures and tables for a clear understanding. Figure 1 displays the approximate solutions of the model for different combinations of β_1 and β_2. As observed, the solution exhibits slower or faster diffusion rates depending on the choice of fractional orders, which reflects the memory effect inherent in fractional derivatives. To further quantify the accuracy of the numerical scheme, the error function was plotted in Figure 2, showing the difference between the exact and numerical solutions over the spatial domain. Additionally, Figure 3 presents a detailed view of the error function at the specific points $y = t = 0.5$, highlighting the pointwise accuracy of the proposed approach. From a physical perspective, this fractional diffusion model can describe anomalous diffusion phenomena observed in many fields, such as contaminant transport in porous media, heat transfer in materials with memory, and particle transport in complex fluids. The fractional orders β_1 and β_2 allow the model to capture sub-diffusive or super-diffusive behavior, which classical integer-order models cannot accurately represent. For different values of the fractional orders β_1 and β_2, the numerical profiles exhibit noticeably different diffusion patterns, where smaller fractional orders lead to slower diffusion and stronger memory effects, while larger values produce smoother solution surfaces with faster propagation behavior. Finally, Table 1 presents a comparison of the error function, convergence order CO_{Time}, and computational times (CPU in seconds) between the proposed method and an existing fast algorithm. The table clearly demonstrates that the proposed scheme achieves high accuracy with efficient computational performance, making it suitable for practical simulations in physics and engineering applications involving multi-term time-fractional diffusion processes. The computed temporal convergence orders CO_{Time} are observed to be close to second order; however, they are not exactly equal to the theoretical value due to the presence of fractional memory effects, nonlocal temporal operators, and discretization-induced accumulation of truncation errors. It is also important to note that the claimed convergence rates are validated numerically but not rigorously proven in a strict asymptotic sense for all parameter regimes. Instead, they reflect observed computational behavior under practical discretization settings. In the practical implementation of the fast SOE technique, the recursive relation (3.3) is updated sequentially at each time level t_n without storing the complete history of all previous solution values. More precisely, for each exponential term τ_j, the history variable is computed by

$$\mathcal{U}^{n}_{history} = \exp\big(-\tau_j \Delta t_{n-1}\big)\mathcal{U}^{n-1}_{history} + \int_{t_{n-1}}^{t_{n-2}} \exp\big(-\tau_j(t_n - y)\big) z(y)\, dy,$$

which allows the memory contribution to be updated recursively using only previously computed quantities. Consequently, instead of requiring the full storage of all past time steps and a computational complexity of order $\mathcal{O}(n^2)$, the SOE-based recursive implementation reduces the computational cost to nearly $\mathcal{O}(n \log n)$, depending on the adopted exponential compression strategy and the number of exponential terms $\mathcal{N}_{exp}$.

4. Conclusion

In this manuscript, we focused on developing a numerical solution for the time-fractional diffusion model of multi-term order that involves the Riesz-space fractional operator. To tackle this complex fractional model, we employed a hybrid numerical approach that discretizes the problem in both time and space directions. In the time direction, the well-known L1 approximation was used to accurately approximate the Caputo fractional derivatives in the proposed model. For the space direction, the Legendre spectral method was applied to approximate the Riesz-space fractional derivatives with high accuracy. Furthermore, we carried out a stability and convergence analysis of the fully discrete scheme to rigorously investigate the mathematical properties of the proposed numerical method. To validate the approach, we implemented the method on a numerical example that demonstrates both the accuracy and efficiency of the scheme. The results confirm that the proposed hybrid method provides a reliable and precise tool for solving multi-term time-fractional diffusion problems with Riesz-space fractional operators.

Declarations

Availability of data and materials. No datasets were generated or analysed during the current study.

Funding. This research received no external funding.

Competing interests. The authors declare that they have no competing interests.

References

[1] M. Abbaszadeh, *Error estimate of second-order finite difference scheme for solving the Riesz space distributed-order diffusion equation*, Appl. Math. Lett., *88* (2019), 179–185.

[2] A. Ansari and M.H. Derakhshan, *Time-space fractional Euler–Poisson–Darboux equation with Bessel fractional derivative in infinite and finite domains*, Math. Comput. Simulat., *218* (2024), 383–402.

[3] Z. Asgari and S.M. Hosseini, *Efficient numerical schemes for the solution of generalized time fractional Burgers type equations*, Numer. Algorithms, *77* (2018), 763–792.

[4] W. Bu, Y. Tang, Y. Wu, and J. Yang, *Finite difference/finite element method for two-dimensional space and time fractional Bloch–Torrey equations*, J. Comput. Phys., *293* (2015), 264–279.

[5] M. Caputo, *Mean fractional-order-derivatives differential equations and filters*, Ann. Univ. Ferrara, *41*(1) (1995), 73–84.

[6] M. Chen and W. Deng, *Discretized fractional substantial calculus*, ESAIM Math. Model. Numer. Anal., *49*(2) (2015), 373–394.

[7] M. Chen and W. Deng, *A second-order accurate numerical method for the space–time tempered fractional diffusion-wave equation*, Appl. Math. Lett., *68* (2017), 87–93.

[8] M.H. Derakhshan, *Stability analysis of difference-Legendre spectral method for two-dimensional Riesz space distributed-order diffusion-wave model*, Comput. Math. Appl., *144* (2023), 150–163.

[9] M.H. Derakhshan, A. Ansari, and M. Ahmadi Darani, *On asymptotic stability of Weber fractional differential systems*, Comput. Methods Differ. Equ., *6*(1) (2018), 30–39.

[10] M.H. Derakhshan and A. Aminataei, *Comparison of homotopy perturbation transform method and fractional Adams–Bashforth method for the Caputo–Prabhakar nonlinear fractional differential equations*, Iran. J. Numer. Anal. Optim., *10*(2) (2020), 63–85.

[11] M.H. Derakhshan and A. Aminataei, *A new approach for solving multi-variable orders differential equations with Prabhakar function*, J. Math. Model., *8*(2) (2020), 139–155.

[12] M.H. Derakhshan, *Numerical solution of a coupled system of fractional order integro differential equations by an efficient numerical method based on the second kind Chebyshev polynomials*, Math. Anal. Contemp. Appl., *3*(4) (2021), 25–40.

[13] M. Derakhshan and Y. Ordokhani, *Efficient numerical approximation of distributed-order fractional PDEs using GL1-2 time discretization and second-order Riesz operators*, Anal. Numer. Solut. Nonlinear Equ., *9*(2) (2025), 203–220.

[14] M.H. Derakhshan, H. Rezaei, and H.R. Marasi, *An efficient numerical method for the distributed order time-fractional diffusion equation with error analysis and stability*, Math. Comput. Simulat., *214* (2023), 315–333.

[15] Y. Dolak and T. Hillen, *Cattaneo models for chemosensitive movement: numerical solution and pattern formation*, J. Math. Biol., *46*(5) (2003), 461–478.

[16] S. Fouladi and H. Mohammadi Firouzjaei, *Local discontinuous Galerkin method for the Riesz space distributed-order Sobolev equation*, Eng. Anal. Bound. Elem., *155* (2023), 38–47.

[17] H. Ghazizadeh, M. Maerefat, and A. Azimi, *Explicit and implicit finite difference schemes for fractional Cattaneo equation*, J. Comput. Phys., *229*(19) (2010), 7042–7057.

[18] U. Habibah, Z.C. Rohman, Y.N. Dewanti, and A.N. Hananti, *Analytical and numerical solutions of the convection-diffusion-reaction equations applying the Differential Transformation Method and the Crank–Nicholson method along with stability analysis and truncation error analysis*, Comput. Methods Differ. Equ., (2025), doi:10.22034/cmde.2025.64919.2958.

[19] M.S. Hadi, M. Lakestani, and B. Nemati Saray, *The wavelet Galerkin method for fractional delay differential equations*, Calcolo, *62*(4) (2025), 48.

[20] Y.Y. Huang, W. Qu, and S.L. Lei, *On τ-preconditioner for a novel fourth-order difference scheme of two-dimensional Riesz space-fractional diffusion equations*, Comput. Math. Appl., *145* (2023), 124–140.

[21] H. Jafari, B.F. Malidareh, and V.R. Hosseini, *Collocation Discrete Least Squares meshless Method for solving Nonlinear Multi-term Time Fractional Differential Equations*, Eng. Anal. Bound. Elem., *158* (2024), 107–120.

[22] J. Jia, H. Wang, and X. Zheng, *A fast algorithm for time-fractional diffusion equation with space-time-dependent variable order*, Numer. Algorithms, *94* (2023), 1705–1730.

[23] Z. Kammappa and A. Awasthi, *Trigonometric cubic b-spline collocation method for time fractional diffusion equation*, Comput. Methods Differ. Equ., (2025), doi:10.22034/cmde.2025.66393.3103.

[24] M. Lakestani and R. Tuntaş, *Efficient solution for multi-delay fractional optimal control problems via cubic B-splines*, Optim. Control Appl. Methods, *46*(6) (2025), 2411–2422.

[25] D. Li, H.L. Liao, W. Sun, J. Wang, and J. Zhang, *Analysis of L1-Galerkin FEMs for time-fractional nonlinear parabolic problems*, Commun. Comput. Phys., *24* (2018), 86–103.

[26] X. Liu and M. Stynes, *Error analysis of a finite difference method on graded meshes for a multiterm time-fractional initial-boundary value problem*, SIAM J. Numer. Anal., *55* (2019), 1057–1079.

[27] H.R. Marasi, M.H. Derakhshan, A. Soltani Joujehi, and P. Kumar, *Higher-order fractional linear multi-step methods*, Phys. Scr., *98*(2) (2023), 024004.

[28] K.S. Miller and B. Ross, *An Introduction to the Fractional Calculus and Fractional Differential Equations*, John Wiley and Sons, New York, 1993.

[29] A.K. Mutashar, M. Lakestani, E. Ashpazzadeh, and B. Han, *Development of novel wavelet-based method to solve a specific class of fractional optimal control problems by the presence of the Caputo–Katugampola fractional derivative*, Appl. Numer. Math., (2026), doi:10.1016/j.apnum.2026.02.009.

[30] Z. Odibat and D. Baleanu, *A new fractional derivative operator with generalized cardinal sine kernel: Numerical simulation*, Math. Comput. Simulat., *212* (2023), 224–233.

[31] K.B. Oldham and J. Spanier, *The Fractional Calculus*, Math. Sci. Eng., Vol. 111, Academic Press, 1974.

[32] I. Podlubny, *An Introduction to Fractional Derivatives, Fractional Differential Equations, to Methods of their Solution and some of their Applications*, Math. Sci. Eng., Vol. 198, Academic Press, 1999.

[33] J. Shen, T. Tang, and L. Wang, *Spectral Methods: Algorithms, Analysis and Applications*, Springer Series in Computational Mathematics, Vol. 41, Springer, Heidelberg, 2011.

[34] R. Singh, A. Singh, S. Kumar, and J. Vigo-Aguiar, *A novel high-order approximation method for higher-dimensional time-fractional reaction-diffusion problems with weak initial singularity*, Comput. Methods Differ. Equ., (2025), doi:10.22034/cmde.2025.61994.2712.

[35] N. Srivastava, A. Singh, Y. Kumar, and V.K. Singh, *Efficient numerical algorithms for Riesz-space fractional partial differential equations based on finite difference/operational matrix*, Appl. Numer. Math., *161* (2021), 244–274.

[36] M. Stynes, E. O'Riordan, and J.L. Gracia, *Error analysis of a finite difference method on graded meshes for a time-fractional diffusion equation*, SIAM J. Numer. Anal., *55* (2017), 1057–1079.

[37] L. Wei, X. Zhang, and Y. He, *Analysis of a local discontinuous Galerkin method for time-fractional advection-diffusion equations*, Int. J. Numer. Methods Heat Fluid Flow, *23*(4) (2013), 634–648.

[38] M. Zayernouri and G.E. Karniadakis, *Discontinuous spectral element methods for time- and space-fractional advection equations*, SIAM J. Sci. Comput., *36*(4) (2014), B684–B707.

[39] J. Zhang and C. Xu, *Finite difference/spectral approximations to a water wave model with a nonlocal viscous term*, Appl. Math. Model., *38* (2014), 4912–4925.

[40] R. Zheng, F. Liu, and X. Jiang, *A Legendre spectral method on graded meshes for the two-dimensional multi-term time-fractional diffusion equation with non-smooth solutions*, Appl. Math. Lett., *104* (2020), 106247.

[41] C. Zhu, B. Zhang, H. Fu, and J. Liu, *Efficient second-order ADI difference schemes for three-dimensional Riesz space-fractional diffusion equations*, Comput. Math. Appl., *98* (2021), 24–39.